Accurate Prediction of Clock Transitions in a Highly Charged Ion with Complex Electronic Structure

C. Cheung[1], M. S. Safronova[1,2], S. G. Porsev[1,3], M. G. Kozlov[3,4], I. I. Tupitsyn[5,6] and A. I. Bondarev[3,6]

[1]*Department of Physics and Astronomy, University of Delaware, Delaware 19716, USA*
[2]*Joint Quantum Institute, NIST and the University of Maryland, College Park, Maryland 20742, USA*
[3]*Petersburg Nuclear Physics Institute of NRC "Kurchatov Institute", Gatchina 188300, Russia*
[4]*St. Petersburg Electrotechnical University "LETI", Prof. Popov Street 5, St. Petersburg 197376, Russia*
[5]*Department of Physics, St. Petersburg State University, Ulianovskaya 1, Petrodvorets, St. Petersburg 198504, Russia*
[6]*Center for Advanced Studies, Peter the Great St. Petersburg Polytechnic University, Polytekhnicheskaja 29, St. Petersburg 195251, Russia*

We develop a broadly applicable approach that drastically increases the ability to predict the properties of complex atoms accurately. We apply it to the case of Ir^{17+}, which is of particular interest for the development of novel atomic clocks with a high sensitivity to the variation of the fine-structure constant and to dark matter searches. In general, clock transitions are weak and very difficult to identify without accurate theoretical predictions. In the case of Ir^{17+}, even stronger electric-dipole ($E1$) transitions have eluded observation despite years of effort, raising the possibility that the theoretical predictions are grossly wrong. In this work, we provide accurate predictions of the transition wavelengths and $E1$ transition rates for Ir^{17+}. Our results explain the lack of observations of the $E1$ transitions and provide a pathway toward the detection of clock transitions. The computational advances we demonstrate in this work are widely applicable to most elements in the periodic table and will allow us to solve numerous problems in atomic physics, astrophysics, and plasma physics.

High resolution optical spectroscopy of highly charged ions (HCI) became the subject of much interest recently due to its novel applications for the development of atomic clocks and in the search for new physics beyond the standard model of elementary particles [1–4]. The HCI optical clock proposals, fundamental physics applications, and experimental progress toward HCI high-precision spectroscopy were recently reviewed in [4]. HCI have numerous optical transitions between long-lived states suitable for clock development with very low uncertainties. These transitions are estimated to reach the 10^{-19} level [5–8]. A particular attraction of HCI clock transitions is their exceptionally high sensitivity to variation of the fine-structure constant α and, subsequently, to dark matter searches [2–4].

In many theories beyond the standard model, in particular those involving light scalar fields that appear naturally in cosmological models, the fundamental constants become dynamical (i.e., varying) [9–14]. If fundamental constants such as α exhibit space-time variation, so do the atomic spectra and the clock frequencies, which are potentially detectable with atomic clocks. The dimensionless factor K quantifies the α-variation sensitivity

$$\frac{\Delta E - \Delta E_0}{\Delta E_0} = K \frac{\alpha - \alpha_0}{\alpha_0}, \qquad (1)$$

where α_0 is the current value of α [15] and ΔE_0 is the clock transition energy corresponding to α_0. Experimentally, the variation of α is probed by monitoring the ratio of two clock frequencies with different values of K. Most of the currently operating atomic clocks have $|K| < 1$, with the Yb^+ octupole transition having the highest $K = -6$ [16]. The HCI transitions allow for much higher sensitivities in which $|K| > 100$, making them particularly attractive candidates for these studies [2–4].

It was shown recently that the coupling of ultralight scalar dark matter to the standard model leads to oscillations of the fundamental constants and therefore may be observed in clock-comparison experiments [11,17,18]. In addition, dark matter objects with a large spatial extent, such as stable topological defects, would lead to transient changes in the fundamental constants that are potentially detectable with networks of clocks [12,19–22]. These recent advances make development of novel clocks with a high sensitivity to these effects particularly exciting. The sensitivity of optical clocks to α variation also makes them sensitive to the light scalar dark matter.

The recent development of quantum logic techniques for HCI spectroscopy in which a cooling ion, such as Be^+, provides sympathetic cooling as well as control and readout of the internal state of the HCI ion [23–25], has made rapid progress in the development of HCI clocks possible.

The spectra of the Pr^{9+} ion were recently measured in an electron beam ion trap [26], and the proposed nanohertz-wide clock line was found toward be 452.334(1) nm.

One of the main remaining stumbling blocks to the development of many HCI clock proposals is the large uncertainties in the theoretical predictions of the clock transitions, particularly in cases with holes in the $4f$ shell (for example, Ir^{16+} and Ir^{17+}) or with a midfilled $4f$ shell (Ho^{14+}). While there are high-precision methods that allow one to reliably predict HCI transitions in ions with 1–4 valence electrons to within a few percent or better [27], the approaches for the $4f$-hole systems are still in the development stage, and theoretical accuracy has not been established. While the magnetic dipole ($M1$) transitions in Ir^{17+} between states of the same parity have been measured to good precision [28], the clock transitions or, in fact, any transitions between opposite parity states have not been identified. These transitions were expected to be observed in recent experiments. Their predicted transition rates [29] were well within the experimental capabilities because $M1$ transitions with much smaller transition rates have been observed. The lack of such observations has raised serious concerns about the accuracy of the theoretical predictions. In this work, we resolve this problem and, for the first time, definitively demonstrate an ability to converge the configuration interaction (CI) in systems with a few holes in the $4f$ shell and place an uncertainty bound on the results. Our results explain the lack of observations of the $E1$ transitions and provide a pathway toward the detection of clock transitions.

We note that this work serves as a basis for an efficient treatment of systems with many valence electrons that can be used for a large variety of applications beyond HCI calculations. Numerous problems in astrophysics and plasma physics require the accurate treatment of systems with many valence electrons, such as Fe. The lack of accurate theoretical predictions creates problems in applications involving almost all lanthanides and actinides, as well as many other open-shell atoms and ions of the periodic table. There are many other applications besides HCI where our results are useful—for example, the development of neutral atom lattice clocks based on the $4f^{14} 6s6p \, {}^3P_0^o - 4f^{13}6s^25d \, (J=2)$ transition in Yb [30,31]. None of the currently existing *ab initio* methods are capable of reliably predicting the atomic properties of this $J=2$ state.

The Ir^{17+} ion has $[1s^2,\ldots, 4d^{10}]$ closed shells and a complicated energy level structure with the $4f^{12} 5s^2$, $4f^{13} 5s$, and $4f^{14}$ low-lying levels shown in Fig. 1. Prior calculations include the CI [3], CI Dirac-Fock-Sturm (CIDFS) [28], Fock space coupled cluster (FSCC) [28], and the COWAN code [32] calculations. There is a reasonable agreement, from a few 100 to 1500 cm^{-1}, for the energy levels of the lowest $4f^{13} 5s$ states as all energies are counted from the ground state, which has the same
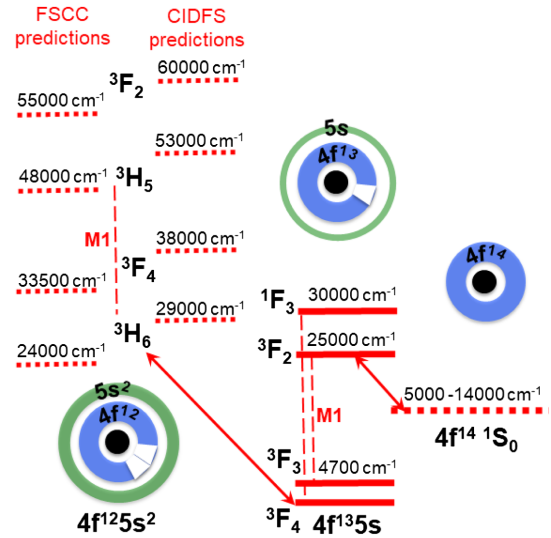

FIG. 1. Low-lying energy levels of Ir^{17+} based on past CIDFS and FSCC calculations [28]. Wavelengths of the three $M1$ transitions shown by the vertical dashed lines have been measured in [28]. The scheme is not to scale.

electronic configuration. However, there are very large, $5000 - 13\,000$ cm^{-1} differences for all other levels. For convenience, we have shown in Fig. 1 the positions of the $4f^{12} 5s^2$ levels predicted using CIDFS [28] and FSCC [28] calculations, which are the most elaborate among all prior approaches. The CI results of [3] place these levels much higher, by $5000 - 7000$ cm^{-1}.

Berengut *et al.* [2] proposed using the $4f^{12} 5s^2 \, {}^3H_6 - 4f^{13}5s^3F_4^o$ transition ($K = -22$) as a clock one. It is an $E3/M2$ transition and can be enhanced via hyperfine-mixing with the ${}^3H_5$ state. They also noted the possibility of using the $4f^{14} {}^1S_0 - 4f^{13} \, 5s \, {}^3F_2^o$ transition, which is $M2$ and may be induced by hyperfine mixing with the $4f^{12} 5s^2 \, {}^3P_1$ level. The particular attraction of this possibility is its very high (predicted to be $K = 143$) sensitivity to the variation of α. Figure 1 illustrates the difficulty in predicting either one of these transition frequencies.

Nine of $M1$ transitions in Ir^{17+} have been experimentally identified and measured at a ppm level [28]. The main puzzle is the lack of observations of two weak $E1$ transitions [29] between the even and odd levels, i.e., the $4f^{12} 5s^2 \, {}^3F_4 - 4f^{13} 5s \, {}^3F_{3,4}^o$ transitions. The theoretical determination of the odd-level splittings is much more reliable compared to the odd-even energy difference, and the observation of the $E1$ transitions would have allowed one to determine the wavelength of the proposed $4f^{12} 5s^2 \, {}^3H_6 - 4f^{13} 5s \, {}^3F_4^o$ clock transition with good precision.

We start from the solutions of the Dirac-Hartree-Fock equations in the central field approximation to construct the one-particle orbitals. We find that the best initial approximation is achieved by solving Dirac-Hartree-Fock equations with the partially filled shells, namely $[1s^2, \ldots, 4d^{10}]4f^{13}5s$.
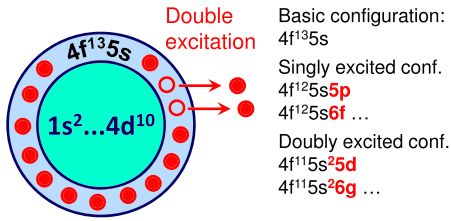
FIG. 2. Single and double excitations from the $4f^{13}5s$ configuration.

FIG. 3. "Opening" the $4d^{10}$ shell—including it into the valence space.

The hybrid approach that incorporates core excitations into the CI by constructing an effective Hamiltonian with the coupled-cluster method [33] cannot be used for this initial approximation. Therefore, the inner shells have to be treated using the CI method, leading to an exponential increase in the number of required configurations. While the weights of most configurations are small, we find the number of important configurations is still very large.

The increased size of the valence space imposes much higher computational demands. To resolve this problem, we develop a message-passing interface (MPI) code that pre-estimates the weights of a very large number of configurations using the perturbation theory (CI-PT approach [34]). We also develop codes to analyze the results and identify and sort the most important configurations. Finally, we develop a fast MPI version of the CI code as the resulting set of important configurations is still extremely large. The new code allowed us to increase the valence space from 24 electrons to all 60 and to include 250 000 configurations, resulting in 133×10^6 Slater determinants, a factor of 20 increase to what was previously feasible.

The CI many-electron wave function is obtained as a linear combination of all distinct states of a given angular momentum J and parity: $\Psi_J = \sum_i c_i \Phi_i$. The energies and wave functions are determined from the time-independent multiparticle Schrödinger equation $H\Psi_n = E_n \Psi_n$.

To definitively ensure the reliability of the theoretical calculations, we consider all possible contributions that may affect the accuracy of the computations and ensure convergence in the following numerical parameters: the number and type of configurations included in the CI, the size of the orbital basis set used to construct the CI configurations, the quantum electrodynamics (QED), and the Breit corrections. We find that by far the largest effect comes from the inclusion of the inner electron shells into the CI, and we studied this effect in detail.

We start with the most straightforward CI computation, which includes single and double excitations from the $4f$ and $5s$ valence shells similar to [3]. This is illustrated in Fig. 2, which shows the first few configurations produced by exciting one and two electrons, starting from the main $4f^{13}5s$ odd configuration. The excitations are allowed to each of the basis set orbitals. We begin with the basis set that includes all orbitals up to $7spdfg$ and discuss the larger basis calculations below.
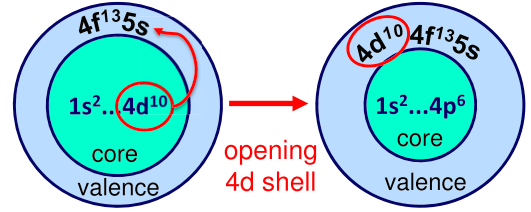
Then, we "open" a $4d$ shell as illustrated in Fig. 3, i.e., we include all $4d$ electrons into the valence space and allow excitations of any of the 24 electrons from the $4d^{10}4f^{13}5s$ shells to the same basis set orbitals up to $7spdfg$. We find drastic changes in the frequencies of all the (odd-even) $E1$ transitions and the position of the $^1S_0$ level. This effect accounts for the difference between the previous CI calculations [3], which prohibited the excitation of the $4d$ electrons, and the CIDFS calculations [28], which allowed such excitation. Because of the large contribution, we continued to include more and more electrons of the inner shells into the CI, up to all 60 electrons. Both single and double excitations are allowed from the $4f$, $4d$, $4p$, $4s$, and $3d$ shells, and single excitations are included for all other shells. We found that the double excitation contribution is small for these inner shells and can be omitted at the present level of accuracy. The results obtained for different numbers of shells included in the CI are given in Table I. We note the very large contribution of the excitation from the $4s$ shell, which is the main source of the difference between our results and the CIDFS calculations [28]. All calculations in Table I are carried out with the same $7spdfg$ basis set.

Three different basis sets of increasing sizes, including all orbitals up to $7spdfg$, $8spdfg$, and $10spdfg$, were used to test the basis set convergence. The differences between the results obtained with the $7spdfg$ and $8spdfg$ basis sets do not exceed 264 cm^{-1} for any level. The difference between the results obtained with the $8spdfg$ and $10spdfg$ basis sets do not exceed 115 cm^{-1} for any level.

We also considered the contribution of the triple excitations from the $5s4f$ shells and found it to be small at the present level of accuracy: -600 cm^{-1} for the $^1S_0$ level and not exceeding -351 cm^{-1} for all other levels. The sum of the corrections for a large $10spdfg$ basis, the triple excitations, the Breit correction beyond the Gaunt term, and the QED corrections [35,36] is given in the column labeled "Other" in Table I. We note that these unrelated corrections substantially cancel each other. Based on the size of the inner shell contributions and all other corrections, we estimate the uncertainties of the final values for the even states to be on the order of 1000 cm^{-1}, which is similar for all states.

The $M1$ transition energies are compared with the experimental values [28] in Table II. Excellent agreement

TABLE I. Energies of Ir^{17+} (in cm^{-1}) obtained using CI with different number of electronic excitations. Only configurations obtained by exciting $4f$ and $5s$ electrons are included in the "$5s4f$ only" column. Excitations from the $4d$ shell are also included in the next column, and the difference of the results is given in the column labeled "$4d$ contribution" The contributions of all other shells are given separately in the next columns. The results for all 60 electrons correlated by the CI are listed in the column "All shells open." The sum of all other corrections is given in the column labeled "Other"—see text for explanation.

Configuration		$5s4f$ only	$5s4f4d$	$4d$ Contribution	$4p$ Contribution	$4s$ Contribution	$3d$ Contribution	$1s2s3s$ Contribution	$3p$ Contribution	$2p$ Contribution	All shells open	Other	Final
$4f^{13}5s$	$^3F^o_4$	0	0	0	0	0	0	0	0	0	0	0	0
	$^3F^o_3$	4714	4745	31	15	14	8	−3	2	0	4781	−4	4777
	$^3F^o_2$	25 170	25 095	−75	14	13	75	−2	25	−4	25 220	−34	25 186
	$^1F^o_3$	30 137	30 253	116	51	33	73	−3	23	−4	30 426	−31	30 395
$4f^{14}$	$^1S_0$	9073	14 870	5797	−931	−1994	1097	−240	−54	9	12 757	−375	12 382
$4f^{12}5s^2$	$^3H_6$	36 362	27 813	−8549	460	1848	−403	183	294	144	30 339	−56	30 283
	$^3F_4$	46 303	37 623	−8680	−5	1858	−410	184	251	144	39 645	−81	39 564
	$^3H_5$	59 883	51 245	−8638	454	1858	−326	183	324	143	53 882	−84	53 798
	$^3F_2$	68 786	60 036	−8751	−188	1690	−384	253	191	64	61 662	−233	61 429
	$^1G_4$	69 099	60 056	−9043	165	1868	−322	184	304	143	62 397	−136	62 261
	$^3F_3$	71 963	63 068	−8894	146	1836	−332	179	266	146	65 309	−129	65 180
	$^3H_4$	91 038	82 254	−8784	78	1894	−245	187	340	142	84 650	−126	84 524
	$^1D_2$	97 473	87 855	−9618	−110	1735	−334	270	177	48	89 639	−366	89 273
	$^1J_6$	109 332	99 131	−10 201	268	1809	−304	171	212	150	101 437	−301	101 136

is observed with the exception of the $^1D_2$–$^3F_3$ transition. It is unclear whether there might be an issue with the experimental identification or if the difference is due to residual electronic correlations. The contribution of the inner shells ($1s$ to $3p$) is particularly large here, about 200 cm^{-1}, which is a factor of 4 larger than for any other $M1$ transition listed in Table II.

The $E1$ transition rates of Ir^{17+} (in s^{-1}) obtained using CI with different numbers of electronic excitations are given in Table III. While opening the $4d$ shell drastically changed the energy levels, we found only a small effect on the matrix elements; the differences in transition rates were caused by differences in energies. When the excitations from the $4p$ shells were included, we found only modest changes in the energies (see Table I) but drastic reductions in the values of the $E1$ matrix elements for a number of

transitions. The multielectron $E1$ transition rates are obtained from the one-body matrix elements, with the appropriate weights based on the mixing of the configurations. Allowing excitations from the $4p$ electrons accounted for the previously omitted $4p$–$5s$ one-electron matrix elements, whose role is particularly important when the contributions from the one-electron $5s$–$5p$ and $4d$–$4f$ matrix elements are close in size but have the opposite sign and essentially cancel each other. The final numbers include the correlations for all 60 electrons. We note that the effect of all other shells for stronger transitions was relatively small.

The previous calculations of the transition rate in Ir^{17+} were only done with FAC code [29] and did not include correlations besides those for the $4f$ and $5s$ electrons. This led to incorrect predictions. In particular, the $^3F_4$–$^3F^o_4$ and

TABLE II. Comparison of Ir^{17+} $M1$ transition energies (in cm^{-1}) with experimental results [28]. The difference (in %) of the other theoretical values (FSCC and CIDFS) from experiment [28] are given in the last two columns.

Transition		Experiment	Present	Difference%	FSCC %	CIDFS %
$4f^{13}5s$	$^3F^o_2$–$^3F^o_3$	20 711	20 409	1.5	1.0	2.6
	$^1F^o_3$–$^3F^o_4$	30 359	30 395	−0.1	0.5	−0.6
$4f^{12}5s^2$	$^3H_5$–$^3H_6$	23 640	23 515	0.5	0.8	1.4
	$^3H_4$–$^1G_4$	22 430	22 263	0.7	0.5	1.9
	$^1G_4$–$^3F_4$	22 949	22 697	1.1	1.2	1.3
	$^1D_2$–$^3F_3$	23 163	24 093	−4.0	−2.0	−5.4
	$^3F_3$–$^3F_4$	25 515	25 616	−0.4	1.0	−0.1
	$^1D_2$–$^3F_2$	27 387	27 844	−1.7	−0.1	−2.0
	$^3H_4$–$^3H_5$	30 798	30 726	0.2	−0.2	1.7

TABLE III. $E1$ $4f^{12}5s^2$–$4f^{13}5s$ radiative transition rates A_{ab} of Ir^{17+} (in s^{-1}) obtained using CI with different numbers of electronic excitations, including excitations from the $4f$ and $5s$ shells, and then adding excitations from the $4d$ and $4p$ shells. The final numbers include the correlations of all 60 electrons. The final values of the transition wavelengths λ (in nm) and reduced $E1$ matrix elements D (in a.u.) are also listed.

Transition	λ	D	Transition rate A_{ab}			
$a-b$			$5s4f$	$+4d$	$+4p$	Final
$^3P_2$–$^3F_3^o$	91	$4.1E-04$	106	111	152	90
$^3P_2$–$^3F_2^o$	112	$9.6E-04$	727	458	276	269
$^3P_2$–$^1F_3^o$	118	$1.2E-03$	1432	1101	254	333
$^3H_4$–$^3F_4^o$	118	$1.6E-03$	798	479	366	358
$^1D_2$–$^3F_3^o$	118	$5.2E-04$	9	4	91	65
$^3H_4$–$^3F_3^o$	125	$1.8E-03$	1325	891	347	369
$^3F_3$–$^3F_4^o$	153	$1.3E-03$	379	201	140	137
$^1D_2$–$^3F_2^o$	155	$9.9E-04$	515	277	103	104
$^1G_4$–$^3F_4^o$	160	$1.8E-03$	677	362	181	184
$^3F_3$–$^3F_3^o$	165	$1.2E-03$	579	319	85	90
$^1D_2$–$^1F_3^o$	169	$1.2E-03$	498	276	105	122
$^1G_4$–$^3F_3^o$	174	$1.7E-03$	376	209	123	129
$^3F_2$–$^3F_3^o$	176	$1.5E-04$	101	60	6	1.7
$^3H_4$–$^1F_3^o$	184	$7.2E-05$	216	0.3	0.2	0.18
$^3F_4$–$^3F_4^o$	252	$4.9E-05$	57	25	0.2	0.03
$^3F_2$–$^3F_2^o$	274	$1.6E-04$	60	26	0.3	0.47
$^3F_3$–$^1F_3^o$	287	$4.3E-04$	48	19	2	2.3
$^3F_4$–$^3F_3^o$	287	$4.9E-04$	64	30	1.2	2.2
$^1G_4$–$^1F_3^o$	313	$1.8E-04$	34	15	0.02	0.2

$^3F_4$–$^3F_3^o$ transition rates, which should have been observable with previous predictions, became extremely small and thus fell well outside the detection range. We identified a number of other transitions for the future $E1$ transition search where the transition rates are above 100 s^{-1}. We have calculated all the $E1$ transitions between the states listed in Table I, including the $^3P_2$ states, but only list the strongest transitions and a few representative examples where the transition rate changes drastically with the opening of the $4p$ shell. (These small values should be considered order-of-magnitude estimates due to large cancellations of different contributions.)

In summary, we have developed a new MPI CI code that allowed us to correlate, for the first time, all 60 electrons in the framework of the CI approach. Our calculations explain the failed search for the $E1$ transitions as follows: the transition rates of the two transitions that were subject to search are well below the detection threshold. We make reliable predictions of the $E1$ and clock transition wavelengths, along with an evaluation of their uncertainties, and provide predictions of the sufficiently strong $E1$ transitions for experimental detection. As illustrated by Table I, the energies of the $E1$ and clock $^3H_6$–$^3F_4^o$ transitions are strongly correlated, and as soon as any of the $E1$ transition

wavelengths is measured, we will be able to establish the clock transition energy with much higher precision.

The method discussed here is very broadly applicable to many elements in the periodic table. Numerous problems in atomic physics, astrophysics, and plasma physics require accurate treatment of the open-shell systems similar to the one considered here. The exceptional speedup of the CI computations demonstrated in this work will allow the computations for other systems where reliable predictions do not yet exist. The present computations were limited only by the computer memory resources presently available to us, and the largest run took fewer than three days on 80 CPUs. The work presented in this Letter, coupled with the development of new methods of efficiently selecting dominant configurations and larger computer resources, will eventually lead to accurate theoretical predictions for most elements of the periodic table.

[1] J. R. Crespo López-Urrutia, Can. J. Phys. **86**, 111 (2008).
[2] J. C. Berengut, V. A. Dzuba, and V. V. Flambaum, Phys. Rev. Lett. **105**, 120801 (2010).
[3] J. C. Berengut, V. A. Dzuba, V. V. Flambaum, and A. Ong, Phys. Rev. Lett. **106**, 210802 (2011).
[4] M. G. Kozlov, M. S. Safronova, J. R. Crespo López-Urrutia, and P. O. Schmidt, Rev. Mod. Phys. **90**, 045005 (2018).
[5] J. C. Berengut, V. A. Dzuba, V. V. Flambaum, and A. Ong, Phys. Rev. A **86**, 022517 (2012).
[6] A. Derevianko, V. A. Dzuba, and V. V. Flambaum, Phys. Rev. Lett. **109**, 180801 (2012).
[7] V. A. Dzuba, A. Derevianko, and V. V. Flambaum, Phys. Rev. A **86**, 054501 (2012).
[8] V. A. Dzuba, A. Derevianko, and V. V. Flambaum, Phys. Rev. A **87**, 029906(E) (2013).
[9] T. Damour and A. M. Polyakov, Nucl. Phys. **B423**, 532 (1994).
[10] J.-P. Uzan, Living Rev. Relativity **14**, 2 (2011).
[11] A. Arvanitaki, J. Huang, and K. Van Tilburg, Phys. Rev. D **91**, 015015 (2015).
[12] Y. V. Stadnik and V. V. Flambaum, Phys. Rev. Lett. **114**, 161301 (2015).
[13] A. Hees, O. Minazzoli, E. Savalle, Y. V. Stadnik, and P. Wolf, Phys. Rev. D **98**, 064051 (2018).
[14] M. S. Safronova, D. Budker, D. DeMille, D. F. J. Kimball, A. Derevianko, and C. W. Clark, Rev. Mod. Phys. **90**, 025008 (2018).
[15] P. J. Mohr, D. B. Newell, and B. N. Taylor, Rev. Mod. Phys. **88**, 035009 (2016).
[16] V. A. Dzuba and V. V. Flambaum, Can. J. Phys. **87**, 15 (2009).

[17] K. Van Tilburg, N. Leefer, L. Bougas, and D. Budker, Phys. Rev. Lett. **115,** 011802 (2015).

[18] A. Hees, J. Guéna, M. Abgrall, S. Bize, and P. Wolf, Phys. Rev. Lett. **117,** 061301 (2016).

[19] A. Derevianko and M. Pospelov, Nat. Phys. **10,** 933 (2014).

[20] P. Wcisło, P. Morzyński, M. Bober, A. Cygan, D. Lisak, R. Ciuryło, and M. Zawada, Nat. Astron. **1,** 0009 (2016).

[21] B. M. Roberts, G. Blewitt, C. Dailey, M. Murphy, M. Pospelov, A. Rollings, J. Sherman, W. Williams, and A. Derevianko, Nat. Commun. **8,** 1195 (2017).

[22] P. Wcisło *et al.*, Sci. Adv. **4,** eaau4869 (2018).

[23] L. Schmöger, O. O. Versolato, M. Schwarz, M. Kohnenand, A. Windberger, B. Piest, S. Feuchtenbeiner, J. Pedregosa-Gutierrez, T. Leopold, P. Micke, A. K. Hansen, T. M. Baumann, M. Drewsen, J. Ullrich, P. O. Schmidt, and J. R. Crespo López-Urrutia, Science **347,** 1233 (2015).

[24] L. Schmöger, M. Schwarz, T. M. Baumann, O. O. Versolato, B. Piest, T. Pfeifer, J. Ullrich, P. O. Schmidt, and J. R. Crespo López-Urrutia, Rev. Sci. Instrum. **86,** 103111 (2015).

[25] P. Micke, T. Leopold, S. A. King, E. Benkler, L. J. Spieß, L. Schmöger, M. Schwarz, J. R. Crespo López-Urrutia, and P. O. Schmidt, Nature (London) **578,** 60 (2020).

[26] H. Bekker, A. Borschevsky, Z. Harman, C. H. Keitel, T. Pfeifer, P. O. Schmidt, J. R. C. López-Urrutia, and J. C. Berengut, Nat. Commun. **10,** 5651 (2019).

[27] M. S. Safronova, V. A. Dzuba, V. V. Flambaum, U. I. Safronova, S. G. Porsev, and M. G. Kozlov, Phys. Rev. Lett. **113,** 030801 (2014).

[28] A. Windberger, J. R. Crespo López-Urrutia, H. Bekker, N. S. Oreshkina, J. C. Berengut, V. Bock, A. Borschevsky, V. A. Dzuba, E. Eliav, Z. Harman, U. Kaldor, S. Kaul, U. I. Safronova, V. V. Flambaum, C. H. Keitel, P. O. Schmidt, J. Ullrich, and O. O. Versolato, Phys. Rev. Lett. **114,** 150801 (2015).

[29] H. Bekker (private communication).

[30] M. S. Safronova, S. G. Porsev, C. Sanner, and J. Ye, Phys. Rev. Lett. **120,** 173001 (2018).

[31] V. A. Dzuba, V. V. Flambaum, and S. Schiller, Phys. Rev. A **98,** 022501 (2018).

[32] U. I. Safronova, V. V. Flambaum, and M. S. Safronova, Phys. Rev. A **92,** 022501 (2015).

[33] M. S. Safronova, M. G. Kozlov, W. R. Johnson, and D. Jiang, Phys. Rev. A **80,** 012516 (2009).

[34] R. T. Imanbaeva and M. G. Kozlov, Ann. Phys. (Berlin) **531,** 1800253 (2019).

[35] V. M. Shabaev, I. I. Tupitsyn, and V. A. Yerokhin, Comput. Phys. Commun. **189,** 175 (2015).

[36] I. I. Tupitsyn, M. G. Kozlov, M. S. Safronova, V. M. Shabaev, and V. A. Dzuba, Phys. Rev. Lett. **117,** 253001 (2016).